# On the Nonlinearities of Inductors using Linear Ferrite Toroidal Cores

J. KENNETH WATSON, SENIOR MEMBER, IEEE

*Abstract*—**The importance of magnetic device characterization as an engineering design tool for inductors and transformers using linear ferrites is emphasized. A piecewise linear model is given for the permeance of a toroidal core, to bring into evidence the role of core geometry on partial saturation under the assumption of an ideally linear core material with abrupt saturation. A variety of measurements are reported for two different inductors under extremes of signal that partially saturate the cores. Measurements and theory are found to agree well only for low-level signals where hysteretic effects are small. At high signal levels the lack of quantitative agreement is attributed to the fact that different features of the hysteresis are probed by the different classes of measurement signals.**

## INTRODUCTION

THE COMMERCIAL availability of linear ferrite cores has facilitated the use of inductors for electronic applications, yet little information is available to explain how they deviate from ideal performance under various conditions of use. No model exists that is capable of providing a detailed picture of the domain configuration, nor of the reversal processes, nor of the large signal current or voltage waveforms that should be expected. Large signal performance is important because of its relation to the engineering problem of minimization of device size, weight, and cost.

Bozorth [1] has carefully reviewed various empirical representations for hysteresis of commercial magnetic materials, but with little emphasis on ferrites that had not yet reached their present commercial importance. Olsen [2] compactly considers ferrites, primarily from the perspective of general principles and careful definitions. Snelling's comprehensive work [3] is still a useful reference that includes a great wealth of data for ferrite cores. This paper seeks to unify three classes of measurements by showing where they agree and where they diverge from one another. The three signal types are ac sinusoids, small sinusoids accompanied by direct current, and unipolar pulses. Toroidal cores were used for these experiments in the belief that the closed toroidal geometry, possessing no airgap, may expose the intrinsic material properties most simply. An ideal model for linear toroidal cores is also given.

An ideal magnetic material for inductors might possess the linear relation $B = \mu H$, where $\mu = \mu_r \mu_0$ is the permeability of the core material which is the product of relative permeability $\mu_r$ and the magnetic content for free space $\mu_0 = 4\pi 10^{-7}$ H/m (MKS units). For toroidal cores that are uniformly wound with $n$ turns, the field due to an applied current $I$,

$$H = nI/2\pi r \quad \text{A} \cdot t/\text{m} \tag{1}$$

is inherently nonuniform at the core, tending to magnetize the inside radius more strongly. If the nonuniformity of induction is taken into account, the total flux in the core is the integral

$$\Phi = \iint B\, ds = \frac{\mu h n I}{2\pi} \int_{r_1}^{r_2} \frac{dr}{r} \quad \text{Wb}/t \tag{2}$$

which leads to the well-known MKS equation for permeance of a toroid

$$P = (\Phi/nI) = (\mu h/2\pi) \ln (r_2/r_1) \quad \text{H}/t^2. \tag{3}$$

In the above derivation, $r_2/r_1/h$ are the outer radius/inside radius/and height in meters. If the nonuniformity of core induction is ignored, the permeance is given by

$$P = \mu S/l_m \quad \text{H}/t^2 \tag{4}$$

where core area $S = h(r_2 - r_1)$ and mean path length $l_m = \pi(r_1 + r_2)$. For most toroid sizes, the theoretical difference is only a few percent between (3) and (4). Equation (4) is also widely used for nontoroidal core shapes. In either event the permeance of a core (sometimes called the $A_L$ factor) defines the inductance $L = n^2 P$ that results from $n$ turns wound upon it. It also follows in the ideal linear case that $L = n\Phi/I$, where the units of flux linkage $n\Phi$ are Webers = voltseconds, and sometimes have the notation $\Lambda = n\Phi$. It may be noted that the same quantity, flux linkage, defines the area under the waveform of voltage induced across the windings of the core.

But our scope of interest includes inductors that may be subjected to large signals and therefore become nonlinear. We make the usual experimental assumption that inductance, permeance and permeability continue to be related to each other by the same constants of turns and geometry as stated above for the ideal case. This assumption has the effect that variations of inductance are exactly proportional to variations in relative permeability. Several kinds of permeability are commonly used to describe core performance [1]–[3]. For purposes of analytical modeling, the present approach considers only part of the nonlinearity problem, that due to saturation of induction, omitting nonlinearities due to hysteresis. For this restricted case there seems to be no ambiguity in defining incremental inductance as the derivative of flux linkage with respect to current

$$L_\Delta = d\Lambda/di \quad \text{H}. \tag{5}$$

Manuscript received August 6, 1980; revised January 5, 1981. An early version of this paper was presented at the 1980 INTERMAG Conference, Boston, MA, April 21–24.

The author is with the California Institute of Technology, 116-81, Pasadena, CA 91125 on leave from the Department of Electrical Engineering, University of Florida, Gainesville, FL 32611.

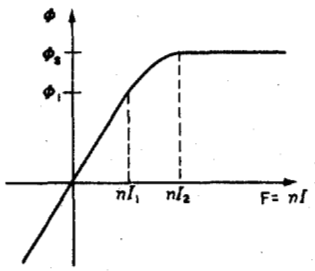


Fig. 1. Calculated curve of flux versus potential for ideal model of saturating but anhysteretic core. Slope of curve defines permeance.

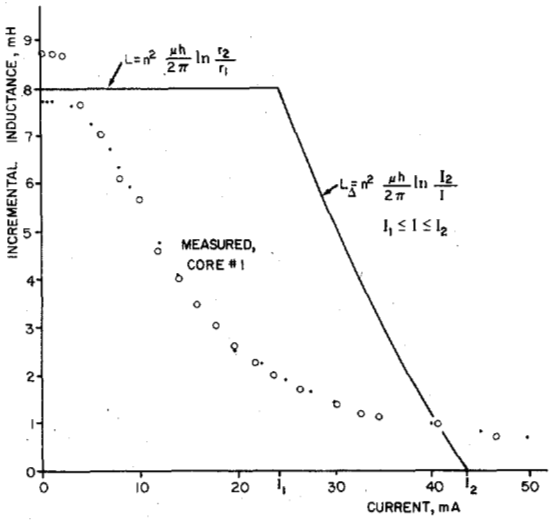


Fig. 2. Calculated incremental inductance for ideal model compared against measured data for core number 1.

It also follows that the induced voltage across an inductor is given by

$$v_L = d\Lambda/dt = (d\Lambda/di) \cdot (di/dt). \tag{6}$$

## Piecewise Linear Model [4]

Let us assume the existence of an ideally linear core material that saturates abruptly at $|B| = B_s$, with negligible hysteresis. If such a material exists, its dominant mode of magnetization change would probably be rotation against a hard-axis anisotropy with little domain wall motion. It follows from (1) that a critical value of current

$$I_1 = B_s 2\pi r_1/n\mu \quad \text{A} \tag{7}$$

corresponds to the onset of saturation at the inner radius of the core. Similarly, $I_2$ defines the current required to saturate the core at the outer radius $r_2$. The curve of $\Phi$ versus $nI$ predicts a gradual saturation of the core, Fig. 1, despite the abrupt saturation of the assumed $B$-$H$ characteristic. The curve of Fig. 1 may be derived by integrating (2) as indicated elsewhere [4].

For the geometry listed below, $(I_2/I_1) = r_2/r_1 = 1.78$ and $(\Phi_1/\Phi_s) = r_1 \ln (r_2/r_1)/(r_2 - r_1) = 0.74$ which suggests that the geometrical effects may be noticeable. The derivative of the curve $d\Phi/d(nI)$ yields (3) for $I < I_1$ and yields

$$P_\Delta = (\mu h/2\pi) \ln (I_2/I) \tag{8}$$

TABLE I
Catalog Data for Two Cores

| quantity | units | Core No. 1 | Core No. 2 |
|---|---|---|---|
| $\mu_i$ | relative | 5000 ± 20% | 2500 ± 25% |
| $A_L$ | $\mu H/t^2$ | 2.75 | 1.38 |
| $B_s$ | T | 0.41 above 4 Oe | 0.5 at 8 Oe |

for $I_1 \leqslant I \leqslant I_2$, which is a new result. Fig. 2 shows the calculated inductance of 50 turns wound on such an ideal core, using the same geometry as the cores in Table I. The value of $\mu_r$ was chosen 16 percent above the nominal value for core no. 1 for good comparison with measured results.

## Coil and Core Details

The measurements described below were made on two toroidal cores of the same size: outside diameter/inside diameter/height = 12.7/7.14/4.77 mm with catalog specifications given in Table I. Mean length/core area $l_m/S$ are given as 2.95 cm/0.128 cm$^2$. Both cores are commercial: no. 1 is a Ferroxcube type 768T188-3E2A, and no. 2 is a TDK type $H_{7C1}$. No effort was made to assure that the responses are typical of the core type because neither endorsement nor criticism is intended. (Two windings of 50 turns each were wound onto each core, with some care taken to distribute the windings uniformly around the circumference.)

## *A-C* Bridge Measurements

Measurements were made of the inductance of each core using an impedance bridge type GR-1650A, which operates at a frequency of 1 kHz and which permits the amplitude of the bridge excitation signal to be varied. Measurements of inductance were made over a range of excitation signals with the results plotted in Fig. 3. It was convenient to use the second 50-turn winding on each core to monitor the voltage. The root-mean-square (rms) voltage across the inductor defines the peak flux linkage by

$$\Lambda_{\text{peak}} = \sqrt{2}\, V_{\text{rms}}/\omega \tag{9}$$

and therefore also defines the peak value of the average induction over the core area by

$$B = \Lambda/nS. \tag{10}$$

The measured value of inductance was found to be sensitive to the value of excitation voltage and generally increased with voltage up to some maximum value. Distortion of the inductor voltage waveform became worse for values above the maximum $L$, indicating that the core was saturating. (The measured quality factor $Q$ of the inductors was noted to be highest at the smallest excitation voltage and decreased sharply to about 6 for core no. 1 (to about 2.7 for core no. 2) for the higher voltages.) Fig. 4 shows the results of a further manipulation of the same data in which $\Lambda$ is now plotted against current, $I_{\max} = \sqrt{2}\, V_{\text{rms}}/\omega L$. The mean value of $H = nI/l_m$ is also shown for reference. The MKS values of $(B; H) = (0.3\ \text{T}; 40\ \text{A} \cdot t/\text{m})$ may also be described by centimeter-gram-second (CGS) values of (3000 G; 0.5 Oe).

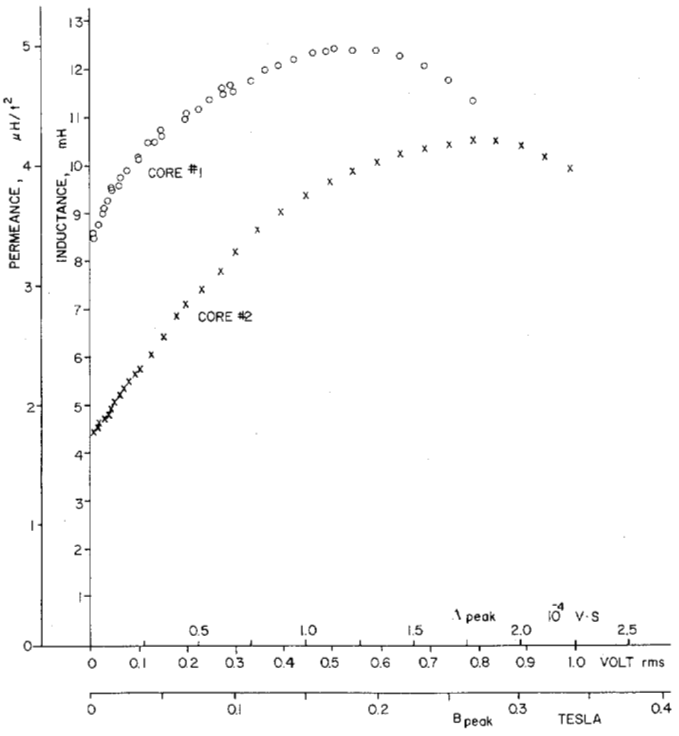


Fig. 3. Impedance bridge measurement of normal inductance with 50 turns on each core, plotted as function of voltage across inductor.

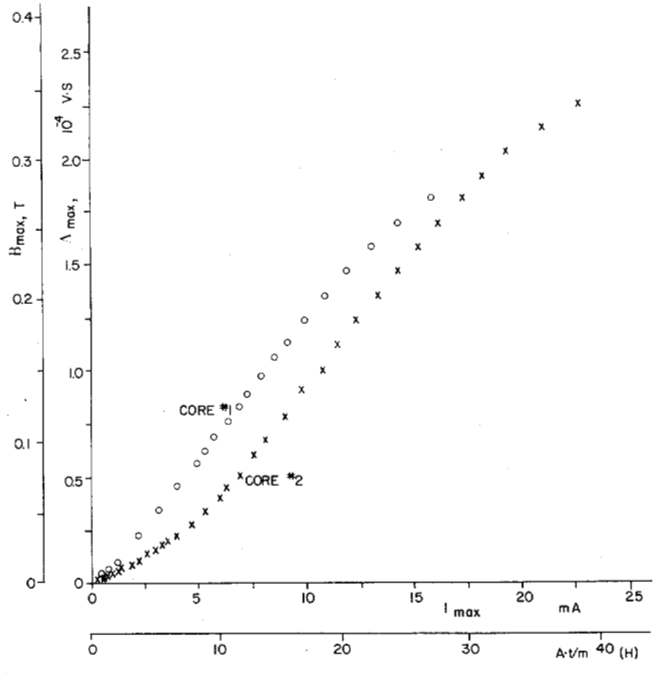


Fig. 4. Same measured data as in Fig. 3, after manipulation into format of Fig. 1.

The type of inductance measured in the above manner is called *normal* inductance, following the definition of normal or amplitude permeability as

$$\mu_a = (1/\mu_0)\, B/H. \tag{11}$$

Amplitude permeability is therefore defined by the slope of a line drawn in Fig. 4 from the origin to a point defined by total $B/H$. It is also clear that $\mu_a$ is proportional to permeance

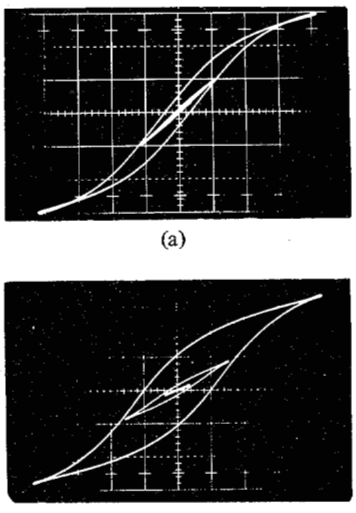


Fig. 5. Hysteresis loops for inductors on core number 1 (top) and core number 2. Each photo is triple exposure of three different loops. Horizontal scale is 5 mA/div. Vertical scale is $0.65 \times 10^{-4}$ V · s/div, hence slope of unity would be inductance of 12.9 mH.

in Fig. 3, so the permeance should be called normal or amplitude permeance. Initial permeability $\mu_i$ is the limiting case of $\mu_a$ for small excitation signals, hence as $B$ and $H$ approach zero.

Normal inductance may also be described as the peak-to-peak slope of a hysteresis loop, as in Fig. 5. As saturation is approached, the bridge measurement definition (which is an average response over a waveform) will diverge from the hysteresis loop definition, since the hysteresis loop includes the details of the distorted waveforms. The opening of the hysteresis loops at higher signal levels indicates an increase of hysteresis loss. This effect corresponds to the decrease of $Q$ noted in the bridge measurements.

## Incremental Inductance

Measurements have been made of core inductance as a function of direct current applied to the second winding of the core. The direct current was controlled by a transistor constant-current circuit in order not to affect the ac bridge measurements at the primary winding. Results for core no. 1 are shown in Fig. 2 for comparison with the piecewise linear model, which is not in good agreement. The measured inductance was found to decrease rapidly as direct current was increased. The measured inductance at low current was found to be sensitive to the amplitude of ac excitation, indicated by two types of data points, but was less so at higher currents. Five mV or less ac voltage[1] was used in most of the measurements, so that a special case of incremental permeability is probably applicable.

General incremental permeability is defined as $\mu_\Delta = (1/\mu_0)\, \Delta B/\Delta H$ without restricting the amplitude of field excursions. The limiting case of reversible permeability,

$$\mu_{rev} = \lim_{\Delta H \to 0} \mu_\Delta \tag{12}$$

[1]Values of voltage and current, for these devices, are related to the average magnetic quantities $B$ and $H$, respectively, as shown by the abscissas of Figs. 3 and 4.

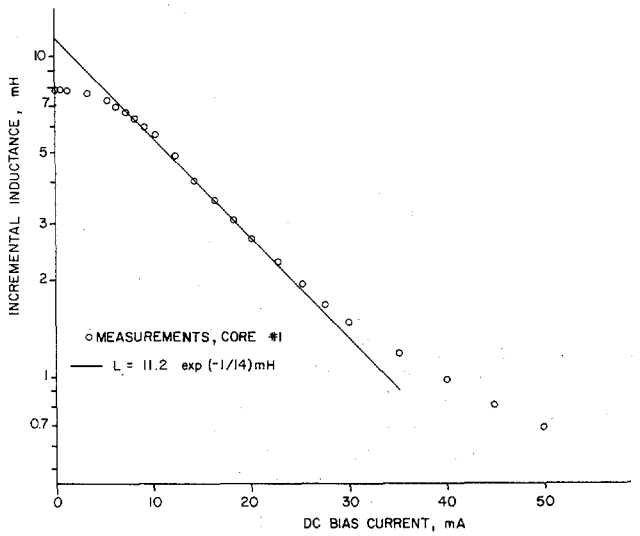


Fig. 6. Incremental inductance for core number 1 plotted on semilog graph.

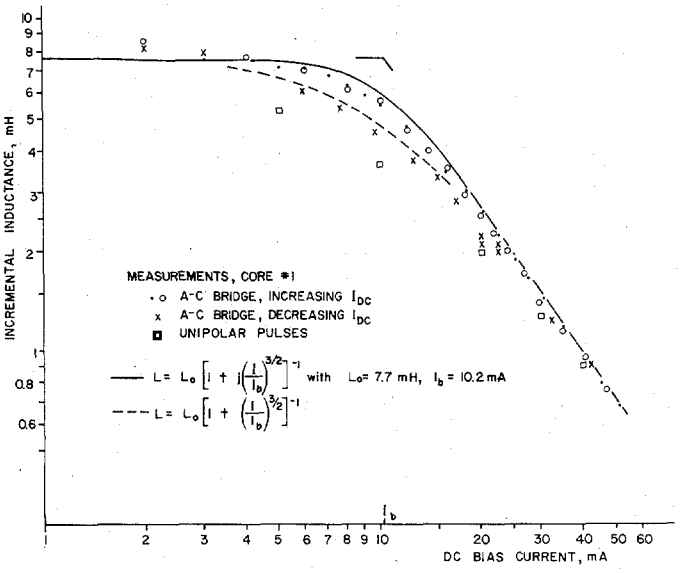


Fig. 7. Incremental inductance for core number 1 plotted on scale of log $L$ versus log $I_{dc}$.

is probably applicable to the present results, but this paper will use the more general terms *incremental* inductance and *incremental* permeability in order to avoid overuse of the letter $r$ subscript that might be confused with relative permeability or recoil permeability.

The measured incremental inductance data was replotted in several ways in an attempt to clarify its meaning. A graph of log $L_\Delta$ versus $I_{dc}$, Fig. 6, has a region of straight line dependence but a physical interpretation is not yet evident. The log-log graph of Fig. 7 reveals several interesting features. The data is suggestive of two regions of operation: a low current region of constant $L$, and a higher current region in which $L$ decreases approximately as $I^{-3/2}$. Data for core no. 2, Fig. 8, has a different exponential dependence. The low current region of constant $L$ has technical importance for power supply filter inductors that carry direct current. The region may be extended, but at a loss of inductance, by introducing an airgap in the core. The high current region of variable inductance might be used to design an electrically tuneable inductor, and it may also have theoretical significance. In the latter connection it is interesting to note that the integral of (5) is approximately

$$\Lambda = \int_0^\infty L\, di \approx \int_0^{i_b} L_0\, di + \int_{i_b}^\infty L_0 (i/i_b)^{-3/2}\, di = 3L_0 i_b \tag{13}$$

which is about 0.9 of the theoretical saturation value for core no. 1.

Physical mechanisms are now proposed to explain these measurements, although it would be risky to regard them as more than speculative with so few data. The measured values of incremental permeability at low direct current agrees with the initial permeability and with the slope of the low amplitude hysteresis loop of Fig. 5, within the accuracy of observation. It is now argued that the small signal measurements probably involve a rotational process. A rotational mode of flux change,

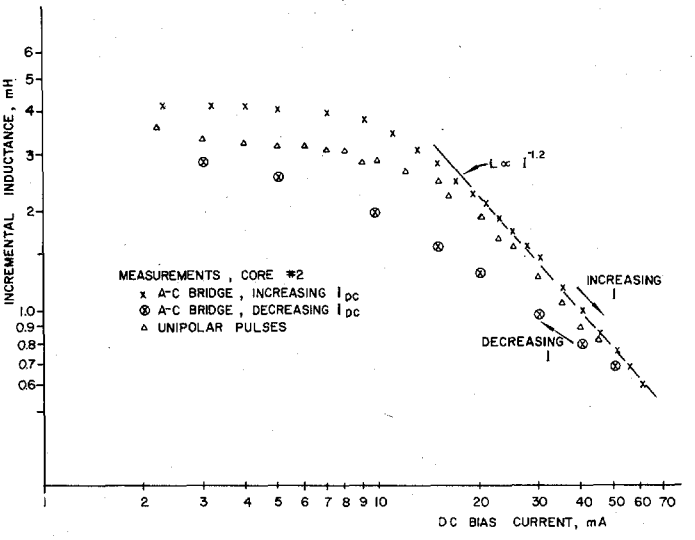


Fig. 8. Incremental inductance data for core number 2.

assuming a uniaxial anisotropy field of

$$H_k = 2K/B_s = B_s/\mu_i\mu_0, \tag{14}$$

yields values of $H_k$ and $K$ of about 54 and 11 for core number 1, and values of 124 and 31 for core number 2. The units of $H_k$ are A$t$/m and of anisotropy constant $K$ are J/m$^3$.

Discussions of initial permeability by Smit and Wijn [5] seem to support an anisotropy model, but with a more complicated physical formula than (14). It is also noted that the arguments given by Bozorth [1, p. 822] for reversible wall motion (for initial permeability of iron and nickel) may not apply to soft ferrites. Elsewhere [1, p. 249] Bozorth notes for a specific ferrite that incremental permeability and crystal anisotropy vary similarly with temperature. Chikazumi [6] discusses reversible processes in some detail. The key question is whether it is reasonable to expect values of $K$ as low as 31 or 11 J/m$^3$.

The mode of reversal seems to change when intermediate values of field are applied to the cores, presumably changing

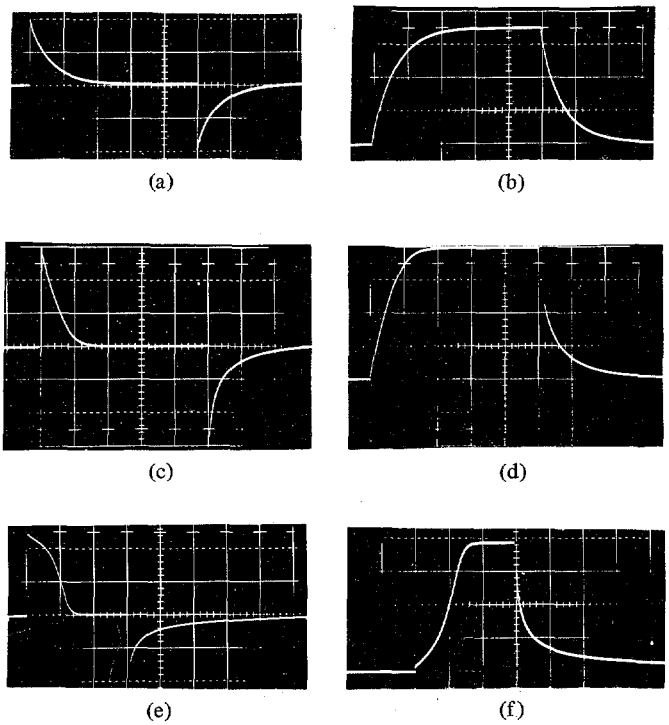


Fig. 9. Voltage (left) and current (right) responses of inductor number 1, in series with 150-Ω resistor, to unipolar voltage pulses of three different amplitudes. Indicated time scale is per division. (a) 0.5 V/div × 100 μs. (b) 2 mA/div × 100 μs. (c) 1 V/div × 100 μs. (d) 5 mA/div × 100 μs. (e) 5 V/div × 20 μs. (f) 20 mA/div × 20 μs.

to wall motion. The hysteresis loops open up, the normal inductances increase significantly, and the incremental inductances begin to decrease. The incremental inductance data seem to support the idea that the small ac field excites only the rotational mode, whereas the direct field establishes the domain configuration. It was observed that measured $Q$ varied with $L_\Delta$ such that the equivalent loss resistance $r = \omega L/Q$ was constant over the entire range of data. It was further observed that measured $L_\Delta$ for *increasing* $I_{dc}$ differed somewhat from the data as $I_{dc}$ was *decreased*, especially for core number 2, Fig. 7. (Care was therefore taken to demagnetize the cores before taking data, then to change $I_{dc}$ only monotonically as measurements were made.)

## Pulsed Inductance

This investigation was stimulated by the observation of current and voltage waveforms, Fig. 9, in a series *R-L* circuit driven by a voltage pulse generator. The character of the waveforms was observed to change with the amplitude of the input pulse in a manner that seemed qualitatively to support the piecewise linear model. Between the exponential decay at low amplitude, Fig. 9(a), and the highly nonlinear response at high amplitude (c), there is observed an intermediate range of amplitudes in which the leading edge of the waveforms possess a distinctive straight line region (b). It is argued subsequently that such a linear ramp current waveform in a series *R-L* circuit implies that the value of inductance decreases linearly with increasing current. It was concluded from further investigations that current and voltage waveforms, such as Fig. 9, are determined by the unipolar pulse inductance. For the cores

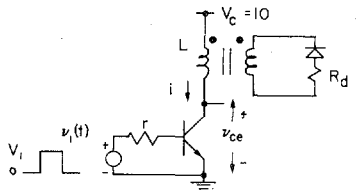


Fig. 10. Circuit for measuring pulse inductance.

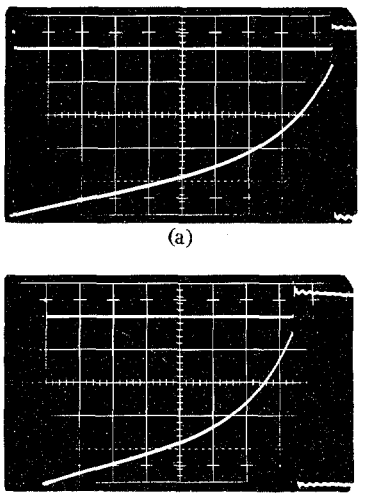


Fig. 11. Inductor current versus time for core number 1 (top) and core number 2. In each photograph upper trace monitors $v_{ce}$ at 20 V/div. to assure that transistor remains saturated. Horizontal scale is 2 μs/div hence may be defined also as $2 \times 10^{-5}$ V · s/div. The vertical scales are (top) 10 mA/div and (bottom) 20 mA/div.

studied, the value of pulse inductance was found to differ from normal inductance, from incremental inductance, and from the piecewise linear model.

Measurements were made of unipolar pulse inductance using the transistor circuit of Fig. 10 as follows. An applied pulse $v_1(t)$ turns on the transistor to saturation so that the voltage across the inductor is approximately equal to the supply voltage

$$v_L = V_c - v_{ce}\,(\text{sat}) \approx V_c \tag{15}$$

where saturation resistance and winding resistance are neglected. The pulse inductance is determined from the rate of rise of current

$$L_p = \frac{v_L}{di/dt} \approx \frac{V_c t}{I} \tag{16}$$

where the right-hand term is valid only in the linear range. Fig. 11 shows the resulting current waveforms, where the increase of slope near the right of each photograph indicates a decrease of inductance as the core approaches saturation. The values for pulse inductance deduced from the linear part of the waveforms are 9 mH for core number 1 and 3.4 mH for core number 2. Pulse permeability may be obtained by working backwards using (3) or (4), in the same manner as for normal permeability or for incremental permeability.

The legend under Fig. 11 points out that the current waveform can be regarded as a graph of $i$ versus $\Lambda$, which is a reoriented version of the magnetization curve $\Lambda$ versus $i$, such

as Figs. 1, 4, or 5. It may be noted that Fig. 11 somewhat resembles a particular portion of the hysteresis curve of Fig. 5, namely the upper trace in the first quadrant. However, a sequence of large amplitude unipolar pulses may drive the core to greater remanence than is indicated by the hysteresis curves of Fig. 5, so pulse inductance may or may not be predicted well by simple measurements of hysteresis. For these cores, pulse permeability is thus believed to be a specific example of *differential* permeability, which indicates the gradient of a hysteresis loop at any specified point [2]

$$\mu_{\text{diff}} = (1/\mu_0)\, dB/dH. \tag{17}$$

Pulsed *incremental* inductance measurements were also made for both cores, with results shown in Figs. 7 and 8. The measurement method consisted of noting the time $T$ required for a voltage transient, such as Fig. 9(a), to decay to half its original amplitude. The inductance was then calculated from the equation

$$L = RT/\ln 2. \tag{18}$$

The results for pulsed incremental inductance were found to agree qualitatively with results for ac incremental inductance. Closer agreement was observed for core number 2, which was attributed to the use of smaller pulses.

## Calculation of Pulsed Response

If a voltage pulse $V$ is applied to an initially quiescent series $R$-$L$ circuit, the transient voltage equation is

$$V = Ri + L(i)\, di/dt \tag{19}$$

where the concept of (5) and (6) are used to define the inductor voltage $v_L$ across the varying inductor $L(i)$. An argument is now given for recognizing the special case of a linearly decreasing range of inductance

$$L(i) = L_0(b - ai) \tag{20}$$

by observing a linearly increasing waveform of current. If there exists a region where $i(t)$ increases linearly, then its derivative $di/dt$ will be constant, where from (19)

$$\frac{di}{dt} = \frac{V - Ri}{L(i)} = \frac{v_L}{L(i)}. \tag{21}$$

But if (21) is a constant, the numerator and denominator of the term on the right must each vary with current in the same way. Since the numerator of the center term explicitly decreases with $i$, it follows that the denominator must also.

No analytical closed solution was found for the nonlinear differential equation that describes the leading edge of the transient, but a numerical solution may be found from the computer integration of

$$T = \int_0^I \frac{L(i)\, di}{V - Ri}. \tag{22}$$

A solution may be calculated for the trailing edge by setting $V = 0$ and the initial value of $i = I_m$ in (22). Alternatively, the trailing edge solution may be found by direct integration of (19), using (20), to yield the result

$$t = \frac{L_0}{R}\left[a(i - I_m) + b \ln (I_m/i)\right]. \tag{23}$$

Equation (23) may be readily solved on a programmable hand calculator to yield values for $t$ for specific values of $I_1 < i < I_m$. This equation was originally solved for the model

$$\begin{aligned} L(i) &= L_0, \quad \text{for } i < I_1 \\ &= L_0\left(\frac{I_2 - i}{I_2 - I_1}\right), \quad \text{for } I_1 < i < I_2 \end{aligned} \tag{24}$$

which thereby defines $a, b$ of (20). Thus $I_m$ must be no larger than $I_2$, and suitable attention must be given to boundary conditions as $i$ decreases through the value $I_1$ at time $t_1$. For $i < I$ the circuit becomes linear by (24) so that the current decays exponentially with time. The total transient is $t_1$ plus the time

$$t = \frac{L_0}{R} \ln\left(\frac{I_1}{i}\right). \tag{25}$$

Waveforms calculated numerically using the above methodology were found to be similar to the measured waveforms of Fig. 9, but lacked close quantitative agreement. It was tentatively concluded that (6) and (22) give a valid formalism for transient calculations of anhysteretic nonlinear inductors, but that improved models are needed for specific inductors.

## Conclusion

This paper has addressed the topic of inductance measurements and their interpretation, specifically applied to nonlinear regions of operation for two inductors wound on different linear ferrite cores. Measurements were made of three definitions of inductance: normal inductance, incremental inductance, and pulse inductance. Quantitative agreement among the measurements was found only at low level signals. The lack of agreement at high signal levels is attributed to hysteretic effects of the core materials, different aspects of which are examined by the different signals used to make the measurements. The analysis contributions of the paper include a piecewise linear model of an ideal inductor that incorporates core saturation but omits hysteresis. There is also a formalism given for the transient analysis of nonlinear inductor circuits.

## Acknowledgment

Partial support by the National Science Foundation and by the University of Florida EIES is gratefully acknowledged. The author thanks Camilla Sieck for assistance with the measurements. Thanks go also to Emil Hozeny for sample cores and to B. B. Ghate for a review of the manuscript.

## References

[1] R. M. Bozorth, *Ferromagnetism.* New York: Van Nostrand, 1951.
[2] E. Olsen, *Applied Magnetism, a study in quantities.* New York: Philips and Spring-Verlag, 1966.
[3] E. C. Snelling, *Soft Ferrites, properties and applications.* London: Butterworths, 1969, also Cleveland CRC Press, 1969; also Kent, England: Newnes-Butterworth.
[4] J. K. Watson, *Applications of Magnetism.* New York: Wiley-Interscience, 1980, pp. 43–44.
[5] J. Smit and H. P. J. Wijn, *Ferrites.* New York: Philips Wiley, 1959.
[6] S. Chikazumi, *Physics of Magnetism.* New York: Wiley, 1964.